

Electronic properties of a UIrGe single crystal

K. Prokeš*

Hahn-Meitner-Institute, NE, Glienickerstrasse 100, D-141 09 Berlin, Germany

T. Tahara, T. Fujita, H. Goshima, and T. Takabatake

Department of Quantum Matter, ADSM, Hiroshima University, Higashi-Hiroshima 739-8526, Japan

M. Mihalik[†] and A. A. Menovsky

Van der Waals-Zeeman Institute, University of Amsterdam, 1018 XE Amsterdam, The Netherlands

S. Fukuda and J. Sakurai

Department of Physics, Toyama University, Gufuku, Toyama 930-8555, Japan

(Received 13 October 1998)

Structural study by means of x-ray powder diffraction and Laue technique show that UIrGe crystallizes in the orthorhombic TiNiSi-type structure. Magnetic measurements reveal a huge magnetic anisotropy in UIrGe with the hard magnetization axis along the a axis, i.e., along the direction of U-U zig-zag chains. Comprehensive magnetic, electrical-transport, thermopower, and thermal studies on a single crystal indicate the magnetic order of UIrGe below 15.8 K with an additional transition at 14.1 K. Magnetic and transport measurements on the polycrystalline sample, however, suggest that UIrGe orders magnetically at 16.4 K. All anomalies shift towards lower temperatures with increasing magnetic field suggesting that an antiferromagnetic ground state takes place in UIrGe at low temperatures. The drastically different low-temperature behavior of the electrical resistivity for single crystal (increasing with decreasing temperature) as compared with that for the polycrystalline sample (electrical resistivity decreases with lowering temperature) suggests different physical properties of bulk and surface areas. Resistivity and thermoelectric measurements indicate that a small gap across a part of the Fermi surface is established in the case of the single crystal. [S0163-1829(99)00237-4]

I. INTRODUCTION

UIrGe belongs to a large group of UTX (T is a late transition metal and X stands for Si or Ge) compounds and up to now has been studied only in polycrystalline form. It crystallizes in the orthorhombic TiNiSi-type structure (space group $Pnma$) where U atoms, which are responsible for magnetic properties, form zig-zag chains running along the a axis.¹

UIrGe represents one of the most puzzling cases among orthorhombic UTX compounds despite the considerable effort of several research groups. All bulk properties which have been studied so far, point to an antiferromagnetic (AF) ordering below 16–18 K. This concerns the anomaly in the temperature dependence of magnetic susceptibility,^{2–4} a sharp peak on the C_p/T vs T curve^{2,5} accompanied by a dramatic reduction of the γ value from 145 to 18 mJ/mol K² across the transition from the high to the low-temperature phase^{2,5} and a dramatic resistivity drop below 17 K.^{1,5,6} The specific-heat anomaly shifts by 0.5 K towards lower temperatures when a field of 5 T is applied.⁵ The conclusion about the AF ground state is furthermore supported by the magnetization curves measured at 4.2 K which exhibit two clear metamagnetic transitions at 13 and 19 T, respectively.⁵ However, no indication of AF order down to 1.5 K has been provided by neutron powder-diffraction experiments so far.^{7–9}

Recently, a single crystal of UIrGe of sufficient quality has been prepared. This opens the possibility of investigating

electronic properties of this compound in a single-crystalline form and to provide valuable information about the magnetic anisotropy. In this paper we report on the electronic properties of single-crystalline UIrGe.

II. EXPERIMENTAL DETAILS

A single crystal of UIrGe has been grown from a stoichiometric melt by a modified Czochralski technique in a continuously gettered purified Ar atmosphere. Materials used in preparation were at least 99.95% pure. No subsequent heat treatment was given to the crystal. The quality of the resulting product was checked by the Laue x-ray technique and by electron microprobe analysis (EPMA). The structural parameters of UIrGe were verified with x-ray powder diffraction. For this purpose, part of the single crystal was ground under an inert atmosphere. We used Cu $K\alpha$ radiation and the diffraction pattern was analyzed by means of the Rietveld refinement program FULLPROF.¹⁰

Magnetic susceptibility $\chi(T) = M/H$ has been measured by means of a superconducting quantum interference device magnetometer (Quantum Design) in fields up to 5 T in the temperature range 2–320 K on a cube-shaped sample, oriented along principal axes by a Laue technique. Magnetization curves along principal axes at various temperatures have been measured by the same magnetometer in fields up to 5.5 T. For the electrical-resistivity measurements, performed by a standard four-probe dc method in the temperature region 4.2–300 K, bar-shaped samples cut along principal

TABLE I. The refined structural parameters of U-Ir-Ge.

Space group:		<i>Pnma</i>	<i>T</i> = 300 K	
U	4(<i>c</i>)	$x_U \frac{1}{4} z_U$	$x_U = -0.00490(61)$	$z_U = 0.20079(30)$
Ir	4(<i>c</i>)	$x_{Ir} \frac{1}{14} z_{Ir}$	$x_{Ir} = 0.21599(48)$	$z_{Ir} = 0.58533(58)$
Ge	4(<i>c</i>)	$x_{Ge} \frac{1}{14} z_{Ge}$	$x_{Ge} = 0.82904(97)$	$z_{Ge} = 0.58566(148)$
Lattice parameters			<i>R</i> factors	
$a = 686.28 \pm 0.02$ pm			$R_p = 6.04\%$	$\chi^2 = 10.6$
$b = 430.16 \pm 0.01$ pm			$R_{wp} = 7.81\%$	
$c = 757.81 \pm 0.02$ pm			$R_B = 5.21\%$	

axes have been used. The typical dimensions were $0.45 \times 0.45 \times 2.5$ mm³. Electrical contacts were established by thin gold wires fixed by a silver paint. The temperature dependence of the specific heat in zero field was measured by a semiadiabatic heat-pulse method between 1.5 and 50 K. The thermoelectric power was measured between 1.5 and 285 K by a standard stationary technique of detecting a small electrical potential difference due to a small temperature gradient across a rectangular bar ($1.2 \times 1.2 \times 5.0$ mm³) cut along the *a* axis.

In view of the rather unexpected results obtained on single crystal, part of the crystal was remelted in order to obtain a polycrystalline sample and some of the experiments were repeated under the very same conditions (x-ray diffraction, electron-probe analysis, magnetic measurements, and electrical resistivity).

III. RESULTS: SINGLE CRYSTAL

A. Sample characterization and crystal structure

Top and bottom parts of the crystal, which had a length of 7 cm and a diameter of 4–5 mm, were inspected by electron microprobe analysis (EPMA). The top part has been found to be single phase and homogeneous with a proper composition. The bottom part of the crystal was found to consist of two phases. The matrix (95 vol. %) was found to be homogeneous with composition deviating from the ideal stoichiometry of UIrGe by no more than 1 at. % (the resolution limit of EPMA). The second phase (5 vol. %) was identified as UIr.¹¹ It has been found that the amount of UIr phase increases towards the bottom of the crystal. Therefore, about 2 cm in length of the crystal was cut from the bottom side and not used in the study. Content of UIr of less than 0.6% was concluded to be present in a used part of the crystal on the basis of magnetic measurements. Moreover, from x-ray Laue technique it follows that our crystal possesses a slight mosaicity in the *a*-*c* plane (about 2–3°) between the main crystallites.

X-ray powder diffraction at room temperature confirmed that UIrGe forms in the orthorhombic TiNiSi-type structure, in agreement with the literature.^{1,3,7,8} In this structure, all the atoms occupy the 4(*c*) crystallographic position but with different position parameters. Structural parameters determined at room temperature, which agree well with the literature,^{1,3,4,7,8} are given in Table I.

B. Magnetic properties

In Fig. 1, the temperature dependence of the inverse susceptibility measured along the principal axes is shown. Above 70 K, the magnetic susceptibility for all three orientations is field independent whereas at low temperatures some deviations occur. Because for lower magnetic fields stronger enhancement of χ is recorded, these deviations are assigned to a certain amount of ferromagnetic UIr, which orders at 46 K.¹¹ The magnetic anisotropy is multiaxial, nearly of an easy-plane type. The hard-magnetization direction is found along the *a* axis, whereas the easy-magnetization axis is found along the *b* direction, except for a small temperature region around 16 K, where it is parallel to the *c* axis (see Fig. 2). Above 100 K, all three $\chi(T)$ curves can be fitted by a modified Curie-Weiss (MCW) law which includes a temperature-independent term χ_0 . The best fits to MCW behavior (in Fig. 1, shown by solid lines) yield effective moments of $\mu_{\text{eff}}^a = 1.26 \pm 0.02 \mu_B/U$, $\mu_{\text{eff}}^b = 2.00 \pm 0.01 \mu_B/U$, and $\mu_{\text{eff}}^c = 1.83 \pm 0.01 \mu_B/U$ for the *a*, *b*, and *c* axis, respectively. For paramagnetic Curie temperatures, values of $\theta_p^a = -77 \pm 2$ K, $\theta_p^b = -16 \pm 1$ K, and $\theta_p^c = -18 \pm 1$ K are obtained. The temperature-independent term χ_0 amounts to about 1.0×10^{-8} m³/mol for all three orientations. The effective moments μ_{eff} derived from MCW fits can be regarded as a lower limit of the real effective moments. However, it should be kept in mind that in the present case, due to a strong magnetic anisotropy, already a very small tilt (or mosaicity) from the desired orientation leads to the necessity

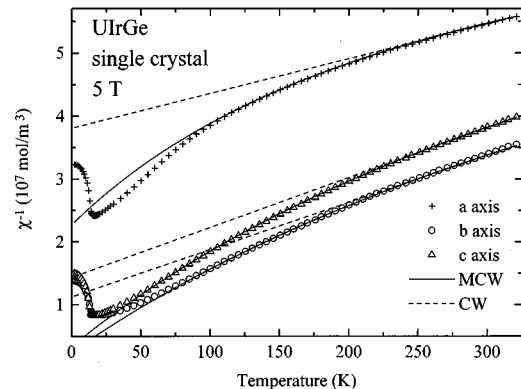


FIG. 1. The temperature dependence of the inverse susceptibility ($\chi = M/H$) measured in field of 5 T applied along the principal axes of a UIrGe single crystal. Solid and broken lines through symbols denote the best fits to MCW and CW behavior, respectively.

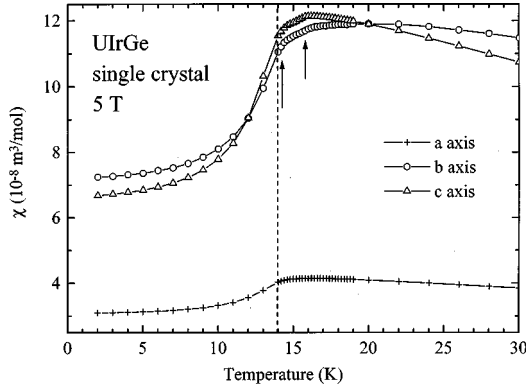


FIG. 2. The low-temperature part of $\chi(T)$ measured in field of 5 T along the principal axes of UIrGe single crystal. The dashed line denotes T_N defined by a maximum in $\partial(T\chi(T))/\partial T$. Arrows denote two anomalies in $\chi(T)$ connected with a change in a slope.

to employ a MCW fit due to a mixing of different CW branches. This affects most seriously the hard-axis data and leads to artificially enhanced χ_0 for all principal directions.

At higher temperatures, it is possible to approximate $\chi(T)$ by a Curie-Weiss law. Above 250 K, fits, which are shown in Fig. 1 by broken lines, yield much higher effective moments of $\mu_{\text{eff}}^a = 3.40 \pm 0.02 \mu_B/U$, $\mu_{\text{eff}}^b = 2.91 \pm 0.01 \mu_B/U$, and $\mu_{\text{eff}}^c = 2.82 \pm 0.01 \mu_B/U$ and paramagnetic Curie temperatures $\theta_p^a = -686 \pm 9$ K, $\theta_p^b = -145 \pm 3$ K, and $\theta_p^c = -179 \pm 4$ K for the a , b , and c axis orientation, respectively. The drastically different paramagnetic Curie temperatures indicate that a strong magnetic anisotropy is present in UIrGe. While the anisotropy in the b - c plane (as determined from the difference of paramagnetic Curie temperatures $|\theta_p^b - \theta_p^c|$ obtained from CW fits) is about 35 K, the anisotropy within the a - b and a - c planes is much stronger. On the other hand, one should realize that at high temperatures (i.e., in the region of CW fits) the magnetic susceptibility is small and therefore the precision of such an analysis is reduced.

In Fig. 2, the low-temperature details of $\chi(T)$ measured in the field of 5 T are shown. Two anomalies (changes in the slope) are present for the b and the c axis orientations. For the a axis only one anomaly (at the maximum) is clearly present. For the field directed along the c axis the relevant temperatures at 5 T are 15.8 and 14.1 K, respectively, and are denoted by arrows. These anomalies shift towards lower temperatures with applied magnetic field. In field of 1 T they appear in the magnetic susceptibility with field along the c axis at 16.1 and 14.5 K, respectively. This result suggests that at low temperatures an antiferromagnetic order appears in UIrGe in agreement with suggestions in literature.¹⁻⁷ However, it is well known that the magnetic ordering temperature T_N in the majority of antiferromagnets cannot be identified with the susceptibility maximum but with the maximum in $\partial(T\chi(T))/\partial T$ which appears for the c -axis orientation in a field of 1 T at 14.0 K and which is in Fig. 2 denoted by a vertical broken line. Additionally, a much smaller maximum in $\partial(T\chi(T))/\partial T$ along the c -axis is visible at 15.8 K. Anomalies for the b -axis orientation exhibit very similar field dependence, whereas the anomaly for the a -axis direction is field invariant.

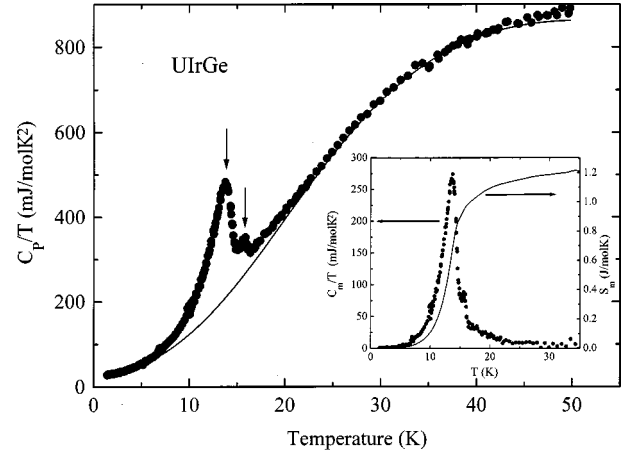


FIG. 3. The temperature dependence of the specific heat of UIrGe in zero field divided by temperature C_p/T . The solid line represents the sum of the electronic contribution (given by the low-temperature specific-heat coefficient $\gamma = 25.69$ mJ/mol K²) and the phonon part approximated by a Debye function with $\theta_D = 182$ K. In the inset, the temperature dependence of the magnetic part of the specific heat divided by temperature together with the magnetic entropy is shown.

The magnetization curves measured along the principal axes in fields up to 5.5 T at several temperatures are linear in field almost at all temperatures. The only exceptions are found in the close vicinity of the transition temperature T_N , i.e., around 15 K, along the b and c axes, where a very small upturn is present. Magnetization along the b and the c axes are considerably higher than for the a -axis direction qualifying the a axis as the hard axis. At low temperatures, a small intercept with the magnetization axis is observed for all orientations. This ferromagnetic signal is due to a small (about 0.5 wt. %) amount of UIr. It disappears above 50 K in agreement with the fact that UIr orders ferromagnetically at 46 K.¹¹

C. Specific heat

In Fig. 3 we show the temperature dependence of the specific heat of UIrGe divided by temperature C_p/T . It is dominated by a pronounced peak centered at 14.1 K and a smaller feature at 15.8 K. Positions of these anomalies agree well with those inferred from magnetic-susceptibility measurements. The heat capacity has been analyzed as the sum of three contributions: the electronic, phonon, and magnetic contributions. The low-temperature part of C_p/T was approximated by the expression $C_p/T = \gamma + aT^2$, where γ denotes the low-temperature specific-heat coefficient and serves as an estimate of the electronic contribution. By fitting the C_p/T curve to $\gamma + aT^2$ between 1.4 and 6 K values of $\gamma = 25.69 \pm 0.15$ mJ/mol K² and $a = 1.125 \pm 0.008$ mJ/mol K⁴ have been obtained. This yields, through the formula $\theta_D^3 = 3 \cdot 12 \pi^4 R / 5a$,¹² where a is the T^2 coefficient, an estimate for the Debye temperature of $\theta_D = 173$ K. However, a much better agreement in both the low- and the high-temperature limit, is obtained with a Debye temperature $\theta_D = 182$ K. The Debye function with the latter θ_D was taken as an estimate for the phonon background. The magnetic contribution, which is shown in the inset of Fig. 3, was then calculated by

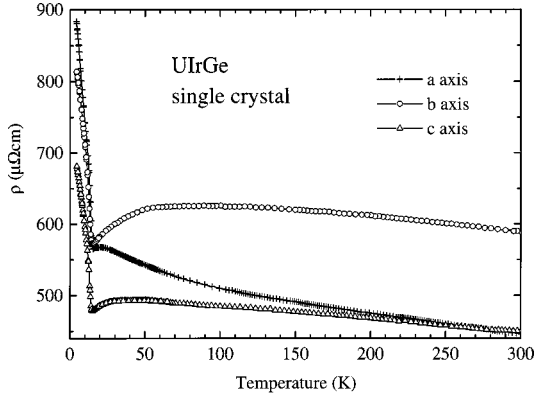


FIG. 4. The temperature dependence of the electrical resistivity $\rho(T)$ in zero field measured with current along the principal axes of single-crystalline UIrGe.

subtracting the phonon and the electronic contributions from the total specific heat. The magnetic entropy, which is obtained by integration of the magnetic part of the specific heat C_m (i.e., the total specific heat minus electronic and lattice contributions) divided by temperatures up to 35 K, yields $S_m = \int dTC_m/T = 0.21R \ln 2$.

It has been pointed out by Ramirez *et al.*² that if the low-temperature specific-heat coefficient γ is determined by linear extrapolation of the high-temperature data C/T vs T^2 above T_N , a much larger value is obtained. Indeed, this procedure leads to $\gamma = 141.4 \pm 3.3$ mJ/mol K² and $a = 0.678 \pm 0.008$ mJ/mol K⁴ from the experimental data between 17 and 22 K. Although this result has only a limited meaning because at this temperature region the phonon background already deviates from T^3 dependence, it suggests that a large portion of the Fermi surface S_{Fermi} is removed at T_N . If a naive picture that $\gamma \propto S_{\text{Fermi}}$ is employed, a reduction by 82% is found to take place. Such a reduction is sometimes observed in antiferromagnetically ordered materials at the magnetic phase transition due to Fermi surface gapping. In this case, also a drastic change in the temperature dependence of electrical resistivity is expected.

D. Electrical resistivity

In Fig. 4, the temperature dependence of the electrical resistivity $\rho(T)$ measured with current along the principal axes is shown. $\rho(T)$ exhibits significant anisotropy. In the high-temperature region it increases along all three principal directions. The increase is more pronounced for the a axis than for the other two orientations. At lower temperatures, the increase gradually flattens and resistivity starts to decrease, for different orientations at different temperatures. Finally, below T_N , the electrical resistivity sharply increases for all three directions. For the b - and c -axis orientations T_N can be estimated to be 14.3 K, in good agreement with magnetic and specific-heat results. For the a axis, however, somewhat higher transition temperature of about 15.1 K can be estimated. At lower temperatures the increase is slower. However, the saturation is not completed down to 4.2 K for neither of the three directions. The $\rho_{4.2\text{K}}/\rho_{300\text{K}}$ ratio amounts to 1.98, 1.39, and 1.51 for the a , b , and c axis orientation, respectively.

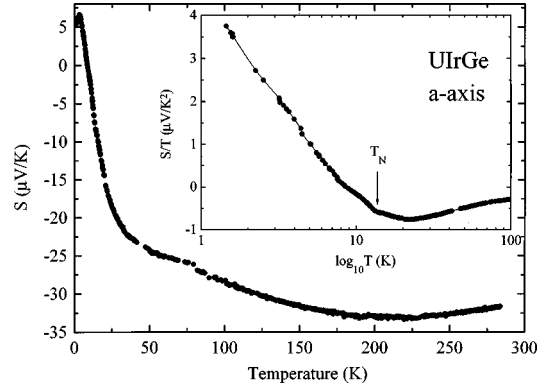


FIG. 5. The temperature dependence of thermoelectric power S of a UIrGe single crystal measured along the a axis. In the inset, the low-temperature part in S/T versus $\ln T$ representation is shown.

This result is surprising because all previous electrical-resistivity measurements on polycrystalline samples revealed a sharp decrease below approximately 17 K, which was suggested as a magnetic phase-transition point. Usually, electrical resistivity for a single crystal is smaller than that for polycrystalline material because of a higher degree of perfection of the lattice and thus lower residual resistivity in the case of the single crystal. It should be, however, noted that below 7 K, also an increase of the polycrystalline electrical resistivity has been reported.^{1-4,6}

E. Thermoelectric power

In Fig. 5, the temperature dependence of the thermoelectric power $S^a(T)$ measured along the a axis is shown. At high temperatures it is flat and exhibits large negative value. Around 220 K $S^a(T)$ shows in an absolute value a maximum and decreases in an absolute value with decreasing temperature. At 9 K it changes its sign and goes through a maximum situated at 3.2 K before falling down at even lower temperatures. Such a maximum is usually interpreted as being due to a temperature-dependent structure at E_F . The magnetic phase transition is situated near the maximum slope of the upturn in $S^a(T)$.

Although the thermoelectric power (TEP) can be expressed as a sum of two contributions, one due to diffusion of electrons and the other due to so-called phonon drag which is a consequence of electron-phonon interaction, we will discuss here only the low-temperature part where the latter contribution plays a minor role (normally, phonon drag if important manifests itself as a maximum at $T \approx \theta_D/5 = 35$ K, which is not the case). The electron diffusion part can be expressed as¹³

$$S = - \frac{\pi^2 k_B^2 T}{3e} \left\{ \frac{\partial \ln N(E)}{\partial E} + \frac{\partial \ln \tau(E)}{\partial E} \right\}_{E=E_F}, \quad (1)$$

where $N(E)$ is the density of states near the Fermi surface, τ denotes the relaxation time of the scattering of conduction electrons, and the other symbols have the usual meaning. As it can be seen from Eq. (1), the diffuse part of the TEP is caused by any change in the conduction process, such as the change of the carrier density or the scattering mechanism. It is also seen that if TEP is not equal to zero in the whole

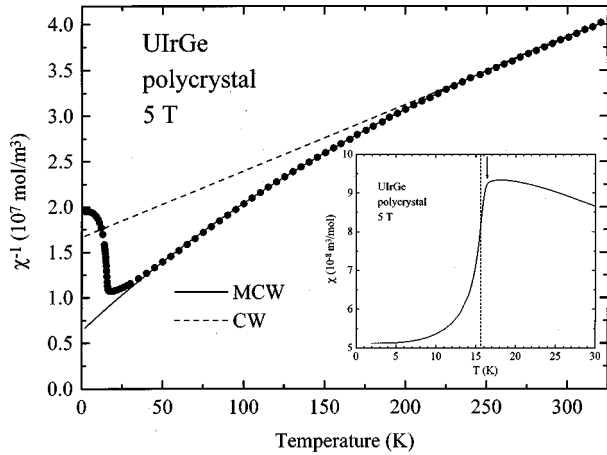


FIG. 6. The temperature dependence of the inverse magnetic susceptibility measured at 5 T on a fine powder sample of UIrGe with grains fixed in random orientations by a glue. The low-temperature part of $\chi(T)$ is shown in the inset.

temperature range it has to exhibit a maximum or minimum because $S(T=0 \text{ K})=0$. Therefore, we show in the inset of Fig. 5 TEP in the S/T versus $\ln T$ representation. In this case, S/T increases at low temperatures without any saturation tendency. Below 7.5 K, this increase is exponential (i.e., S/T versus $\ln T$ is a straight line) and resembles the TEP of semiconductors.

IV. POLYCRYSTALLINE STUDIES

An unexpected increase in $\rho(T)$ along all three principal directions for the single crystal of UIrGe has motivated our further study on polycrystalline samples. The polycrystal, used for structural, magnetic, and electrical-transport measurements under the very same conditions as in the case of the single crystal, has been prepared by remelting part of the single crystal under protective purified Ar atmosphere. It was flipped and remelted three times to obtain a good homogeneity. Finally, the electrical arc has been switched off without decreasing the current.

The structural study by means of powder x-ray diffraction led to the same structure, including cell and positional parameters. Also the electron microprobe analysis did not reveal different composition with respect to the single crystal.

In Fig. 6, the temperature dependence of the inverse magnetic susceptibility measured at 5 T on a fine powder fixed by a weakly diamagnetic glue, together with the best MCW and CW fits made in the same temperature regions (as in the case of a single crystal), is shown. The fitted parameters are $\mu_{\text{eff}}=1.83\pm 0.01\mu_B/U$, $\theta_p=-38\pm 1 \text{ K}$, and $\chi_0=1.0\times 10^{-8} \text{ m}^3/\text{mol}$ in the case of a MCW fit and $\mu_{\text{eff}}=2.95\pm 0.01\mu_B/U$, $\theta_p=-228\pm 1 \text{ K}$ for a CW fit at high temperatures. These results are in very good agreement with values obtained on polycrystals.¹⁻⁴ In the inset of Fig. 6, we show the low-temperature part of the polycrystalline $\chi(T)$ curve. In this case, only one abrupt change in the slope can be seen. It shifts from 16.8 K in 1 T to 16.3 K in 5 T. Also the maximum in the temperature derivative of $\partial(T\chi(T))/\partial T$, which can be associated with T_N , shifts slightly towards lower temperatures from 16.4 K in 1 T to 15.7 K at 5 T (in

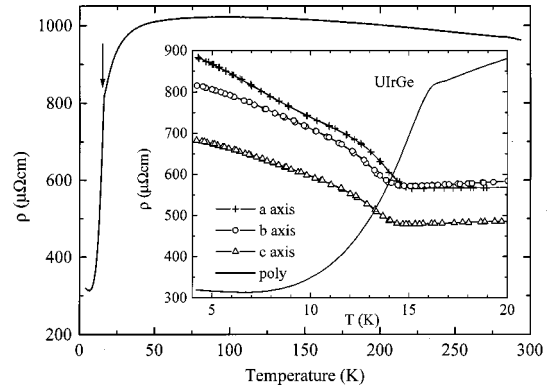


FIG. 7. The temperature dependence of the electrical resistivity measured on the polycrystalline sample of UIrGe. Comparison with single-crystal data in the low-temperature region is shown in the inset.

the inset of Fig. 6 indicated by a broken line for 1 T). Direct comparison with results obtained on a single crystal (see Fig. 1) reveals that the all anomalies in the case of single-crystal data appear 1–2 K below those in polycrystal. Magnetization curves at various temperatures measured on a polycrystalline sample are nearly straight lines and show, except for absolute values, the same behavior as magnetization curves measured on a single crystal.

In Fig. 7, the temperature dependence of the electrical resistivity measured on the polycrystalline sample under the same conditions as in the case of the single crystal is shown. It slightly increases with lowering the temperature, goes through a very flat maximum at 100 K and decreases at lower temperatures. The slope changes abruptly and $\rho(T)$ drops sharply below 16.4 K marking the onset of magnetic ordering. The decrease amounts to 60% of the resistivity value at 16.4 K. However, below 7 K $\rho(T)$ starts to increase with further lowering of the temperature and the $\rho_{4.2 \text{ K}}/\rho_{300 \text{ K}}$ amounts to 0.33. Such temperature behavior of $\rho(T)$ was reported for the UIrGe polycrystal independently by several groups.^{1-4,6} In the inset of Fig. 7 we show the low-temperature part of the temperature dependence of the electrical resistivity combining polycrystalline and single-crystalline data. As can be seen, the absolute value of $\rho(T)$ measured on the polycrystal is above T_N , higher than the $\rho(T)$ values obtained in the case of the single crystal. At low temperatures the situation is interchanged. The drop in the resistivity of the polycrystal occurs at higher temperature than the increase of the $\rho(T)$ curves obtained in the case of the single crystal.

V. DISCUSSION

Structural studies confirmed that UIrGe forms in the orthorhombic TiNiSi-type structure, which is the ternary-ordered variation of the CeCu₂ type. The structural parameters are in good agreement with literature values.^{1,3,4,7,8} In this structure, U atoms, which are thought to be mainly responsible for magnetic properties, form zig-zag chains running along the *a* axis. The shortest U-U separation which amounts to 351.18 pm is found within the chains whereas the next-nearest-neighbor distance is given by the separation of chains and amounts to 372.6 pm. The former (latter) distance

is comparably (larger) than Hill's critical distance of 350 pm,¹⁴ and one can expect rather delocalized $5f$ electron states in UIrGe. Moreover, the shortest U-Ir (289.2 pm) and U-Ge (295.0 pm) distances suggest that the $5f$ -ligand hybridization contributes significantly to delocalization and coupling mechanisms. From all these facts one can expect a huge magnetic anisotropy in UIrGe. Indeed, the anisotropy energy expressed in terms of a difference in the paramagnetic Curie temperatures deduced from CW fits is enormously high. While the anisotropy in the b - c plane is about 35 K, the anisotropy within the a - b and a - c planes reaches several hundreds of Kelvins. The strength of the anisotropy found in UIrGe is common in uranium compounds^{15,16} and its type is very similar to that found in UNiGe (the only other system with $X = \text{Ge}$ studied in a single-crystalline form).¹⁶⁻¹⁸ The fact that the effective magnetic moments are smaller than those for $5f^3$ or $5f^2$ configurations even if deduced from high-temperature parts (by CW fits) of $\chi(T)$ can be taken as an argument that $5f$ states in UIrGe are significantly delocalized.

Magnetic measurements in the paramagnetic region yield results that are in good agreement with literature dealing with polycrystalline data,¹⁻⁴ whereas at low temperatures the agreement is not complete. In particular, the magnetic phase transition on a single crystal is found in the present study at lower temperatures, namely at 14.1 K. However, lower T_N than published values¹⁻⁶ is found only in the case of the single crystal and not in the case of the polycrystalline sample. Moreover, an additional small anomaly at 15.8 K is found on the single crystal. The lower anomaly appears in the specific heat to be about 20 times bigger than that at the higher temperature. The position of the latter peak correlates well with a very sharp λ anomaly published by Buschow *et al.* for the polycrystalline sample.⁵ The low-temperature specific-heat coefficient γ amounts to $\gamma = 25.69 \pm 0.15$ mJ/mol K² that is a value higher by 6–12 mJ/mol K² than literature.^{2,5} By an extrapolation of data above T_N , however, a much higher value for γ is obtained suggesting that a large portion of the density of states at the Fermi surface is removed due to Fermi-surface gapping. The magnetic entropy released at 35 K ($S_m = 0.21R \ln 2$) suggests that magnetism in UIrGe is governed by strongly delocalized $5f$ electrons.

The largest difference with respect to previous polycrystalline results^{1,5,6} has been found in electrical transport properties measured on a single crystal. This concerns both the magnetic phase transitions and the tendency of the resistivity below this transition.

One can argue that the different magnetic and electrical transport properties are due to small ferromagnetic UIr. However, from magnetization measurements it follows that the amount of UIr in our sample is small and that the polycrystalline sample, which was prepared from the single crystal, shows a similar distribution of UIr. A more probable explanation is that the physical properties of surface and bulk regions are very different. Let us suppose that various structural defects accumulating at grain boundaries in the case of the polycrystal induce internal stresses and cause the electronic structures of the surface (less perfect structure) and bulk areas (more perfect structure) to be different. A small energy gap at E_F which would cause the electrical resistivity

to increase with lowering the temperature and which would lead to a low density of states $n(E_F)$ at E_F can be established in the single crystal. Such a possibility is supported by fully relativistic optimized linear combination of atomic orbitals calculations by Diviš *et al.*¹⁶ which include spin and orbital polarizations. These calculations reveal that E_F is situated at the edge of the $5f$ band at a local minimum of the density of states. Different electronic structures also imply that the Stoner product $In(E_F)$, where I denotes the exchange interaction, is different for bulk and surface regions and consequently it leads to different ordering temperatures. With this assumption, it seems to be possible to explain the double transition in the case of the single crystal, and different electrical transport properties of the single crystal with respect to the polycrystal. Our single crystal possesses slight mosaicity, i.e., a certain part of our single crystal belongs to the surface areas between grains. Therefore, two transitions are present in the C_p/T vs T curve, the larger at lower temperature belonging to the bulk and the smaller at higher temperature to surface regions. The polycrystalline sample, on the other hand, should exhibit predominantly the upper transition, which is also observed and reported in the literature.^{1-6,15}

If surface areas exhibit at low temperatures lower resistivity than the bulk region it is possible also to explain the difference in the electrical resistivity between the single crystal and the polycrystal. The size of the drop (or size of the increase in the case of the single crystal) at low temperatures is then expected to be strongly dependent on the distribution of grain boundaries in the sample. If these boundaries establish a continuous path (which happens in the polycrystalline sample), a decrease of $\rho(T)$ at low temperatures should be observed. If it does not exceed the percolation limit (likely to be the case in the single crystal), an increase in $\rho(T)$ should appear at low temperatures.

Opening of an energy gap at the Fermi surface in the case of the more perfect lattice of the single crystal is supported by the reduction of the γ value below T_N which suggests that a large portion of the Fermi surface disappears at T_N (in $5f$ electron systems with a shortest U-U distance falling into the Hill's critical region,¹⁴ one would on the contrary expect high γ values due to the formation of a highly correlated $5f$ band at the Fermi level). It seems that the gap is not uniform across E_F and some connecting nodes exist as it is documented by the temperature dependences of thermopower, specific heat, and electrical resistivity measured on a single crystal. For instance, the electrical resistivity is far from being of the activation type found in semiconductors. It resembles the electrical resistivity of FeSi,^{19,20} albeit the rise is in an absolute scale much smaller in our sample. Moreover, an averaging of the Fermi surface in the case of a polycrystal would contribute to a big difference in $\rho(T)$ with respect to the single crystal.

Although we have shown that the electronic properties of polycrystalline and single crystalline UIrGe are different at low temperatures, more elaborate studies, involving detailed electronic structure calculations are needed.

VI. CONCLUSIONS

We report on the electronic properties of UIrGe single crystal. Structural studies confirmed that UIrGe adopts the

orthorhombic TiNiSi-type structure. Magnetic measurements reveal a huge magnetic anisotropy of UIrGe. The hard magnetization axis was found to be along the a axis. Comprehensive bulk measurements suggest that two magnetic phase transitions, at 14.1 and 15.8 K, are present in single-crystalline UIrGe. Resistivity and magnetic-susceptibility measurements on a polycrystalline sample prepared by arc melting from the single crystal reveal only the upper magnetic transition which is situated at 16.4 K. All anomalies shift towards lower temperatures with increasing magnetic field, suggesting that an antiferromagnetic ground state exists in UIrGe at low temperatures. The drastically different low-temperature behavior of the electrical resistivity on the single crystal with respect to previously published data taken on polycrystalline samples^{1-6,15} (and our measurements ob-

tained on polycrystalline samples), suggest different magnetic and transport properties of bulk and surface areas between grains.

ACKNOWLEDGMENTS

This work was sponsored by the Japanese Society for the Promotion of Science (JSPS), by a Grant-in-Aid for Scientific Research from the Ministry of Education, Science, Sports, and Culture of Japan (Mombusho), and by the "Stichting voor Fundamenteel Onderzoek der Materie" (FOM). We would like to thank S. Shibata, the Instrument Center for Chemical Analysis, Hiroshima University for EPMA measurements.

*On leave from: Department of Electronic Structures, Charles University, 12116 Prague 2, Czech Republic.

†Permanent address: Institute of Experimental Physics, Slovak Academy of Sciences, 043 54 Košice, Slovak Republic.

¹B. Chevalier, B. Lloret, P. Gravereau, B. Buffat, and J. Etourneau, *J. Magn. Magn. Mater.* **75**, 13 (1988).

²A. P. Ramirez, B. Batlogg, and E. Bucher, *J. Appl. Phys.* **61**, 3189 (1987).

³R. Troć and V. H. Tran, *J. Magn. Magn. Mater.* **73**, 389 (1988).

⁴B. Chevalier, E. Hickey, and J. Etourneau, *J. Magn. Magn. Mater.* **90&91**, 499 (1990).

⁵K. H. J. Buschow, E. Brück, R. G. van Wierst, F. R. de Boer, L. Havela, V. Sechovský, P. Nozar, E. Sugiura, M. Ono, M. Date, and A. Yamagishi, *J. Appl. Phys.* **67**, 5215 (1990).

⁶V. H. Tran, R. Troć, and B. Badurski, *J. Magn. Magn. Mater.* **87**, 291 (1990).

⁷V. H. Tran, R. Troć, F. Bourée, T. Roisnel, and G. André, *J. Magn. Magn. Mater.* **140-144**, 1377 (1995).

⁸V. H. Tran, F. Bourée, G. André, and R. Troć, *Solid State Commun.* **98**, 111 (1996).

⁹R. A. Robinson, H. Nakotte, F. R. de Boer, K. H. J. Buschow, V. Sechovský, L. Havela, and A. Purwanto, MLNSC-LANSCE, Progress report, 1993 (unpublished).

¹⁰J. Rodrigues-Carvajal, FULLPROF version 3.2 Jan97 (unpublished).

¹¹A. Dommann, F. Hulliger, T. Siegrist, and P. Fisher, *J. Magn. Magn. Mater.* **67**, 323 (1987).

¹²See, for instance, N. W. Ashcroft and N. D. Mermin, in *Solid State Physics*, edited by R. W. Cahn, P. Haasen, and E. J. Kramer (CBS Publishing ASIA Ltd, Philadelphia, 1988), p. 459.

¹³See, for instance, B. Coqblin, *The Electronic Structure of Rare-Earth Metals and Alloys: The Magnetic Heavy Rare-Earths* (Academic, London, 1977), p. 605.

¹⁴H. H. Hill, in *Plutonium 1970 and Other Actinides*, edited by W. N. Miner (AIME, New York, 1970), p. 1.

¹⁵V. Sechovský and L. Havela, in *Ferromagnetic Materials*, edited by E. P. Wohlfarth and K. H. J. Buschow (North-Holland, Amsterdam, 1988), Vol. 4, p. 309.

¹⁶M. Diviš, M. Richter, and M. Olšovec (unpublished); see Fig. 2.1 in V. Sechovský and L. Havela, in *Handbook of Magnetic Materials*, edited by K. H. J. Buschow (North-Holland, Amsterdam, 1998), Vol. 11, p. 7.

¹⁷K. Prokeš, H. Nakotte, E. Brück, F. R. de Boer, L. Havela, V. Sechovský, P. Svoboda, and H. Maletta, *IEEE Trans. Magn.* **30**, 1214 (1994).

¹⁸H. Nakotte, I. H. Hagmusa, J. C. P. Klaasse, M. S. Torikachvili, A. H. Lacerda, E. Brück, K. Prokeš, and F. R. de Boer, *Physica B* **246-247**, 441 (1998).

¹⁹M. B. Hunt, M. A. Cernikov, E. Felder, H. R. Ott, Z. Fisk, and P. Canfield, *Phys. Rev. B* **50**, 14 933 (1994).

²⁰D. Mandrus, J. L. Sarrao, A. Migliori, J. D. Thompson, and Z. Fisk, *Phys. Rev. B* **51**, 4763 (1995).